SCIENTIFIC BULLETIN
OF
THE POLITEHNICA UNIVERSITY OF TIMISOARA

Vol.66(80)	MATHEMATICS–PHISYCS	2021

ON THE DYNAMICS OF A DEFORMED VERSION OF THE SHIMIZU-MORIOKA SYSTEM

Cristian LĂZUREANU, Jinyoung CHO

Abstract

In this paper, we construct a family of integrable deformations of the Shimizu-Morioka chaotic model. We discuss the stability of a particular deformed system which belongs to this family and we emphasize its chaotic behavior. We also perform some numerical simulations in order to show the transition to chaos and the deformation of the chaotic attractor.[1]

1 Introduction

The real life phenomena are often modeled by systems of first order differential equations. Particularly, phenomena with chaotic behavior are widely investigated (see, e.g., [1, 3, 28, 31]) and many chaotic systems were introduced and discussed (see, e.g., [2, 4, 35, 36, 37, 40]). In 1963, Lorenz reported the first chaotic system, so called the Lorenz model [27]. In 1980, Shimizu and Morioka introduced a more tractable model which displays similar dynamics as the Lorenz system [34]. A simplified form of the Shimizu-Morioka system is given by

$$\begin{cases} \dot{x} = y \\ \dot{y} = x - \lambda y - xz \\ \dot{z} = -az + x^2 \end{cases}, \tag{1}$$

where $a, \lambda \in \mathbb{R}$.

System (1) has been investigated from the dynamical point of view, see for instance a partial list of references: chaotic behavior [33, 41], control of chaos [30, 6], bifurcations [38, 26], integrability [11], Jacobi stability [39].

[1]MSC(2010): 37D45, 70H05
Keywords and phrases: *Hamilton-Poisson systems, integrable deformation, stability, chaotic systems.*

BUPT

Recently, integrable deformations of some Hamilton-Poisson systems were discussed (see, e.g., [7, 10, 14, 15, 18, 21, 22, 23, 24]). Moreover, the integrable deformations method for a three-dimensional system of differential equations [16] was applied to some dissipative systems [17, 19, 20]. In this paper, we will apply the above-mentioned method to system (1).

The paper is organized as follows. In Section 2, we construct some integrable deformations of system (1). Then we consider a particular deformation which has the same divergence as the initial system and the same axis of symmetry. In Section 3, we discuss the stability of the new system. More precisely, we get the equilibrium points taking into account the variation of the parameters. Then, we study the stability of the isolated hyperbolic equilibrium points by using the first Lyapunov's stability criterion [25] and Routh-Hurwitz theorem [8]. Also, we establish the stability of the isolated non-hyperbolic equilibrium points by computing the first Lyapunov coefficient (see, e.g., [13]). In Sections 4 and 5, we perform some numerical simulations and point out the chaotic behavior of the considered deformed system.

2 Integrable Deformations of the Shimizu-Morioka system

In this section, we construct some deformation of the Shimizu-Morioka system. Deformations of the system are obtained by using the integrable deformations method for three dimensional systems of differential equations [16].
System (1) writes

$$\dot{\mathbf{x}} = \mathbf{f}(\mathbf{x}),$$

where $\mathbf{x} = (x, y, z) \in \mathbb{R}^3$ and $\mathbf{f}(\mathbf{x}) = (y, x - \lambda y - xz, -az + x^2)$. We choose the vector fields $\mathbf{g}(\mathbf{x})$ and $\mathbf{h}(\mathbf{x})$ such that $\mathbf{f}(\mathbf{x}) = \mathbf{g}(\mathbf{x}) + \mathbf{h}(\mathbf{x})$ and the system $\dot{\mathbf{x}} = \mathbf{g}(\mathbf{x})$ has two functionally independent constants of motion $H = H(\mathbf{x})$ and $C = C(\mathbf{x})$, that is

$$\nabla H \times \nabla C \neq \mathbf{0}, \dot{H} = \dot{C} = 0.$$

We have

$$\mathbf{g}(\mathbf{x}) = (y, x, 0) \ , \quad \mathbf{h}(\mathbf{x}) = (0, -\lambda y - xz, -az + x^2).$$

The system $\dot{\mathbf{x}} = \mathbf{g}(\mathbf{x})$, that is

$$\begin{cases} \dot{x} = y \\ \dot{y} = x \\ \dot{z} = 0 \end{cases},$$

has the constants of the motion

$$H(x, y, z) = z \ , \quad C(x, y, z) = \frac{1}{2}x^2 - \frac{1}{2}y^2.$$

BUPT

It is easy to see that $\mathbf{g}(\mathbf{x}) = \nabla H \times \nabla C$. Hence an integrable deformation of system (1) is given by [16]

$$\dot{\mathbf{x}} = \nabla \tilde{H} \times \nabla \tilde{C} + \mathbf{h}(\mathbf{x}), \tag{2}$$

where $\tilde{H} = H + \alpha$, $\tilde{C} = C + \beta$ and α, β are arbitrary differentiable functions on $\mathbb{R}^3$. Therefore, we obtain the following result.

Proposition 2.1. *Let α, β be arbitrary differentiable functions on $\mathbb{R}^3$. Then a family of integrable deformations of system (1) is given by*

$$\begin{cases} \dot{x} = y - \beta_y + y\alpha_z + \alpha_y\beta_z - \alpha_z\beta_y \\ \dot{y} = x - \lambda y - xz + \beta_x + x\alpha_z - \alpha_x\beta_z + \alpha_z\beta_x \\ \dot{z} = -az + x^2 - y\alpha_x - x\alpha_y + \alpha_x\beta_y - \alpha_y\beta_x \end{cases} \tag{3}$$

where $a, \lambda \in \mathbb{R}$ and $f_x := \dfrac{\partial f}{\partial x}$.

Particular families of integrable deformations are obtained by choosing the deformation function $\alpha = 0$, that is (3) becomes

$$\begin{cases} \dot{x} = y - \beta_y \\ \dot{y} = x - \lambda y - xz + \beta_x \\ \dot{z} = -az + x^2 - y\alpha_x - x\alpha_y \end{cases}.$$

Also, if $\beta = 0$, then we obtain

$$\begin{cases} \dot{x} = y + y\alpha_z \\ \dot{y} = x - \lambda y - xz + x\alpha_z \\ \dot{z} = -az + x^2 - y\alpha_x - x\alpha_y \end{cases}.$$

We consider the deformation functions $\alpha = \dfrac{g}{2}z^2$ and $\beta = 0$. System (3) becomes

$$\begin{cases} \dot{x} = y(1 + gz) \\ \dot{y} = x - \lambda y + (g-1)xz \\ \dot{z} = -az + x^2 \end{cases}, \ a, \lambda, g \in \mathbb{R}. \tag{4}$$

The first dynamical properties of the above system are given by the next two remarks.

Remark 2.2. *Notice that system (4) has the same divergence as the initial system (1), namely*

$$\nabla \cdot \mathbf{f} = -(a + \lambda).$$

Therefore, if $a + \lambda > 0$, then both systems are dissipative. A dissipative system has "a state space volume that decreases on average along the trajectory so that the orbit approaches an attractor of measure zero in the state space" [36]. In the case of three-dimensional dissipative dynamical systems, these attractors are stable foci, limit cycles, attracting 2-tori, or strange chaotic attractors (see, e.g., [12]).

BUPT

Remark 2.3. *Shimizu-Morioka system* (1) *is invariant under the transformation* $(x, y, z) \to (-x, -y, z)$*, thus the* z*-axis is its axis of symmetry. System* (4) *has the same property. Therefore, a symmetrical orbit or a pair of symmetrical orbits corresponding to symmetrical initial conditions appear in the dynamics of these systems. In addition, the number of the equilibrium points is odd.*

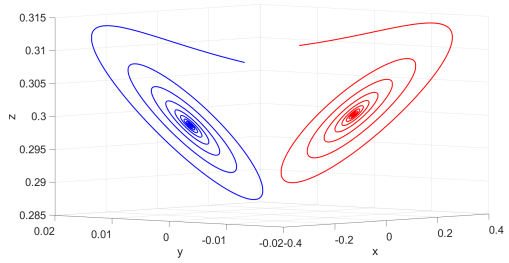


Figure 1: A pair of symmetric stable foci attractors E_1^- and E_1^+, for $a = 0.34$, $\lambda = 0.77$, $g = -2.34$, with initial conditions $x_0 = x(E_1^-) - 0.01$, $y_0 = y(E_1^-) - 0.01$, $z_0 = z(E_1^-) + 0.01$ (blue) and $x_0 = x(E_1^+) + 0.01$, $y_0 = y(E_1^+) + 0.01$, $z_0 = z(E_1^+) + 0.01$ (red) respectively.

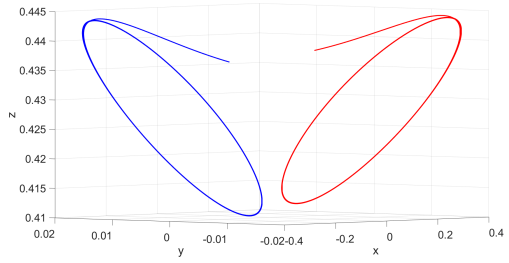


Figure 2: A pair of symmetric limit cycles around E_1^- and E_1^+, for $a = 0.34$, $\lambda = 0.77$, $g = -1.34$, with initial conditions $x_0 = x(E_1^-) - 0.01$, $y_0 = y(E_1^-) - 0.01$, $z_0 = z(E_1^-) + 0.01$ (blue) and $x_0 = x(E_1^+) + 0.01$, $y_0 = y(E_1^+) + 0.01$, $z_0 = z(E_1^+) + 0.01$ (red) respectively.

System (1) displays some types of the above-mentioned attractors. In Figures 1 and 2 are presented pairs of symmetric stable foci and symmetric stable limit cycles respectively. Also, a symmetric limit cycle is shown in Fig. 3, and a chaotic attractor is plotted in Fig. 9.

In the sequel, we will study the stability of the chaotic behavior of system (4).

BUPT

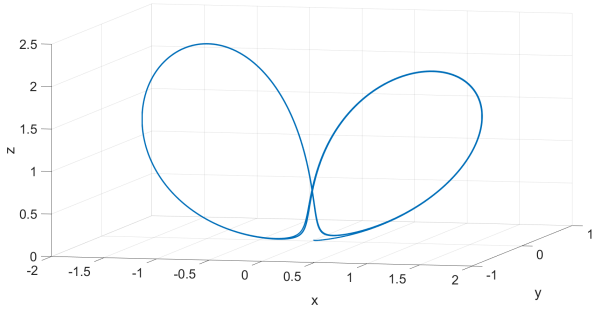


Figure 3: A symmetric limit cycle around E_1^- and E_1^+, for $a = 0.8$, $\lambda = 1$, $g = 0.14$, with initial conditions $x_0 = 0.01$, $y_0 = 0.01$, $z_0 = 0.01$.

3 Stability

In this section, the equilibrium points of the system (4) are identified, and the stability of these equilibrium points is analyzed.

An equilibrium point of the system $\dot{\mathbf{x}} = \mathbf{f}(\mathbf{x})$ is a stationary point of the system, that is that solution which fulfills the condition

$$(\dot{x}(t), \dot{y}(t), \dot{z}(t)) = (0, 0, 0), \forall t \in \mathbb{R}.$$

Then the equilibrium points of the system (4) are the solutions of the system

$$\begin{cases} y(1+gz) = 0 \\ x - \lambda y + (g-1)xz = 0 \\ -az + x^2 = 0 \end{cases} . \tag{5}$$

By solving system (5), we obtain the following equilibrium points of system (4).

Proposition 3.1. *Let* $a,\ \lambda,\ g \in \mathbb{R}$.

1. *If* $a \neq 0,\ \lambda \neq 0,\ g \notin \{0; 1\},\ \dfrac{a}{1-g} < 0,\ \dfrac{a}{g} > 0$, *then the equilibrium point is* $O(0, 0, 0)$.

2. *If* $a \neq 0,\ \lambda \neq 0,\ g \notin \{0; 1\},\ \dfrac{a}{1-g} > 0,\ \dfrac{a}{g} > 0$, *then the equilibrium points are* $O(0, 0, 0)$ *and* $E_1^{\pm}\left(\pm\sqrt{\dfrac{a}{1-g}}, 0, \dfrac{1}{1-g}\right)$.

3. *If* $a \neq 0,\ \lambda \neq 0,\ g \notin \{0; 1\},\ \dfrac{a}{1-g} < 0,\ \dfrac{a}{g} < 0$, *then the equilibrium points are* $O(0, 0, 0)$ *and* $E_2^{\pm}\left(\pm\sqrt{-\dfrac{a}{g}}, \pm\dfrac{1}{\lambda g}\sqrt{-\dfrac{a}{g}}, -\dfrac{1}{g}\right)$.

BUPT

4. *If* $a \neq 0$, $\lambda \neq 0$, $g \notin \{0;1\}$, $\dfrac{a}{1-g} > 0$, $\dfrac{a}{g} < 0$, *then the equilibrium points are* $O(0,0,0)$, $E_1^{\pm}$, *and* $E_2^{\pm}$.
5. *If* $a > 0$, $\lambda \neq 0$, $g = 1$, *then the equilibrium point is* $O(0,0,0)$.
6. *If* $a < 0$, $\lambda \neq 0$, $g = 1$, *then the equilibrium points are* $O(0,0,0)$ *and* $E_2^{\pm}$.
7. *If* $a > 0$, $\lambda \neq 0$, $g = 0$, *then the equilibrium points are* $O(0,0,0)$ *and* $E_1^{\pm}$.
8. *If* $a < 0$, $\lambda \neq 0$, $g = 0$, *then the equilibrium point is* $O(0,0,0)$.
9. *If* $a \neq 0$, $\lambda = 0$, $g = 1$, *then the equilibrium point is* $O(0,0,0)$.
10. *If* $a \neq 0$, $\lambda = 0$, $g \neq 1$, $\dfrac{a}{1-g} < 0$, *then the equilibrium point is* $O(0,0,0)$.
11. *If* $a \neq 0$, $\lambda = 0$, $g \neq 1$, $\dfrac{a}{1-g} > 0$, *then the equilibrium points are* $O(0,0,0)$ *and* $E_1^{\pm}$.
12. *If* $a = 0$, $\lambda = 0$, $g = 0$, *then the equilibrium points are* $E^M(0,0,M)$, $M \in \mathbb{R}$.
13. *If* $a = 0$, $\lambda = 0$, $g \neq 0$, *then the equilibrium points are* $E^M(0,0,M)$ *and* $E^N\left(0, N, -\dfrac{1}{g}\right)$, $M, N \in \mathbb{R}$.
14. *If* $a = 0$, $\lambda \neq 0$, *then the equilibrium points are* $E^M(0,0,M)$, $M \in \mathbb{R}$.

In the following we study the stability of the isolated equilibrium points obtained above. We begin with the stability of $O(0,0,0)$.

Proposition 3.2. *For every* $a, \lambda, g \in \mathbb{R}$ *the equilibrium point* $O(0,0,0)$ *is unstable.*

Proof. The jacobian matrix of system (4) at $O(0,0,0)$ is

$$J(0,0,0) = \begin{pmatrix} 0 & 1 & 0 \\ 1 & -\lambda & 0 \\ 0 & 0 & -a \end{pmatrix}.$$

The characteristic polynomial is

$$P(\mu) = -(\mu + a)(\mu^2 + \lambda\mu - 1)$$

with eigenvalues

$$\mu_1 = -a, \ \mu_2 = \frac{-\lambda - \sqrt{\lambda^2 + 4}}{2}, \ \mu_3 = \frac{-\lambda + \sqrt{\lambda^2 + 4}}{2}.$$

We observe that $\mu_3 > 0$ for all $a, \lambda, g \in \mathbb{R}$. Therefore $O(0,0,0)$ is an unstable equilibrium point. □

BUPT

In the next result we present the stability of the equilibrium points $E_2^{\pm}$.

Proposition 3.3. *If* $a \neq 0$, $\lambda \neq 0$, $g \neq 0$, $\dfrac{a}{g} < 0$, *then the equilibrium points* $E_2^{\pm}\left(\pm\sqrt{-\dfrac{a}{g}}, \pm\dfrac{1}{\lambda g}\sqrt{-\dfrac{a}{g}}, -\dfrac{1}{g}\right)$ *are unstable.*

Proof. The jacobian matrix of system (4) at E_2^- and E_2^+ is

$$J(E_2^{\pm}) = \begin{pmatrix} 0 & 0 & \pm\dfrac{1}{\lambda}\sqrt{-\dfrac{a}{g}} \\ \dfrac{1}{g} & -\lambda & \mp(1-g)\sqrt{-\dfrac{a}{g}} \\ \pm 2\sqrt{-\dfrac{a}{g}} & 0 & -a \end{pmatrix}.$$

The characteristic polynomial for both equilibrium points is

$$P(\mu) = -(\mu+\lambda)\left(\mu^2 + a\mu + \frac{2a}{\lambda g}\right)$$

with eigenvalues

$$\mu_1 = -\lambda,\ \mu_2 = \frac{1}{2}\left(-a - \sqrt{a^2 - \frac{8a}{\lambda g}}\right),\ \mu_3 = \frac{1}{2}\left(-a + \sqrt{a^2 - \frac{8a}{\lambda g}}\right).$$

1. If $\lambda < 0$, then $\mu_1 > 0$. Thus, the equilibrium points $E_2^{\pm}$ are unstable.
2. If $\lambda > 0$, then $\mu_1 < 0$ and $\mu_{2,3} \in \mathbb{R}$. We observe that $\mu_3 > 0$ for all $a, \lambda, g \in \mathbb{R}^*$. Therefore, $E_2^{\pm}$ are unstable equilibrium points, as required.

□

In the last theorem we discuss the stability of the equilibrium points $E_1^{\pm}$.

Theorem 3.4. *Let* $a \neq 0$, $\lambda \in \mathbb{R}$, $g \neq 0$, $\dfrac{a}{1-g} > 0$.

(i) If $\left[a + \lambda > 0,\ a\left(\lambda^2 + a\lambda - \dfrac{2}{1-g}\right) > 0\right]$, *then the equilibrium points* $E_1^{\pm}$ *are asymptotically stable.*

(ii) If $\left[a > 0,\ \lambda > 0,\ \lambda^2 + a\lambda - \dfrac{2}{1-g} = 0,\ l_1(0) < 0\right]$, *then the equilibrium points* $E_1^{\pm}$ *are weak asymptotically stable.*

BUPT

(iii) If $(a+\lambda \leq 0)$ *or* $(a\lambda < 0)$ *or* $\left[a>0,\ \lambda>0,\ \lambda^2+a\lambda-\dfrac{2}{1-g}<0\right]$ *or* $(a>0, \lambda=0)$ *or* $\left[a>0,\ \lambda>0,\ \lambda^2+a\lambda-\dfrac{2}{1-g}=0,\ l_1(0)>0\right]$, *then the equilibrium points* $E_1^{\pm}$ *are unstable.*

The first Lyapunov coefficient $l_1(0)$ *is given by* (9).

Proof. The jacobian matrix of system (4) at E_1^- and E_1^+ is

$$J(E_1^{\pm})=\begin{pmatrix} 0 & \dfrac{1}{1-g} & 0 \\ 0 & -\lambda & \mp\sqrt{a(1-g)} \\ \pm 2\sqrt{\dfrac{a}{1-g}} & 0 & -a \end{pmatrix},$$

with the characteristic equation

$$\mu^3+(a+\lambda)\mu^2+a\lambda\mu+\frac{2a}{1-g}=0. \tag{6}$$

We denote $a_1=a+\lambda$, $a_2=a\lambda$, $a_3=\dfrac{2a}{1-g}$, whence $a_1a_2-a_3=a\left(\lambda^2+a\lambda-\dfrac{2}{1-g}\right)$. By hypothesis, $a_3>0$. Using the Routh-Hurwitz theorem (see, e.g., [8]), we obtain following results:

1. If $a+\lambda>0$ and $a\left(\lambda^2+a\lambda-\dfrac{2}{1-g}\right)>0$, then the characteristic equation (6) has all roots with negative real part. It follows that $E_1^{\pm}$ are asymptotically stable equilibrium points.

   Hence, (i) is proved.

2. If $a+\lambda<0$ or $a\lambda<0$, then the characteristic equation (6) has at least one root with real part strictly positive. Therefore, the equilibrium points $E_1^{\pm}$ are unstable.

3. If $a+\lambda>0$, $a\lambda>0$, and $a\left(\lambda^2+a\lambda-\dfrac{2}{1-g}\right)<0$, then the characteristic equation (6) has a negative real root and a pair of complex conjugate roots with a positive real part. Thus, the equilibrium points $E_1^{\pm}$ are unstable.

4. If $a+\lambda=0$, then the characteristic equation (6) has at least one root with real part strictly positive. It follows that the equilibrium points $E_1^{\pm}$ are unstable.

BUPT

5. If $a > 0$ and $\lambda = 0$, then the characteristic equation (6) has at least one root with a positive real part. Consequently, the equilibrium points $E_1^{\pm}$ are unstable.

Hence, the statement (iii) is proved, less the last condition.

Now, let $a \in \mathbb{R}^*, \lambda, g \in \mathbb{R}$ be such that

$$a + \lambda > 0,\ a\lambda > 0,\ a\left(\lambda^2 + a\lambda - \frac{2}{1-g}\right) = 0.$$

Then $a > 0, \lambda > 0$ and $g = 1 - \dfrac{2}{\lambda(a+\lambda)}$. Moreover, the characteristic equation (6) has the eigenvalues $\mu_1 = -(a+\lambda)$, $\mu_{2,3} = \pm i\sqrt{a\lambda}$.

In this case, there exist a negative real eigenvalue and a pair of purely imaginary eigenvalues. Therefore, the stability of E_1^- is analyzed by applying the procedures proposed by Kuznetsov [13].

First, we translate the equilibrium point E_1^- into origin. Under the transformation

$$\begin{cases} x = X - \sqrt{\dfrac{a}{1-g}} \\ y = Y \\ z = Z + \dfrac{1}{1-g} \end{cases},$$

system (4) becomes

$$\begin{cases} \dot{X} = Y\left(gZ + \dfrac{1}{1-g}\right) \\ \dot{Y} = -\lambda Y + \sqrt{a(1-g)}Z + (g-1)XZ \\ \dot{Z} = -aZ + X^2 - 2\sqrt{\dfrac{a}{1-g}}X \end{cases}. \tag{7}$$

The eigenvectors corresponding to eigenvalues $\mu_1 = -(a+\lambda)$, $\mu_2 = -i\sqrt{a\lambda}$, $\mu_3 = i\sqrt{a\lambda}$ are:

$$v_1 = \left(1, -\frac{2}{\lambda}, \sqrt{\frac{2a(a+\lambda)}{\lambda}}\right),$$

$$v_2 = \left(1, \frac{-2i}{a+\lambda}\sqrt{\frac{a}{\lambda}}, -(\sqrt{a} + i\sqrt{\lambda})\sqrt{\frac{2\lambda}{a+\lambda}}\right),$$

$$v_3 = \left(1, \frac{2i}{a+\lambda}\sqrt{\frac{a}{\lambda}}, -(\sqrt{a} - i\sqrt{\lambda})\sqrt{\frac{2\lambda}{a+\lambda}}\right).$$

BUPT

We define the vectors

$$T = Re(v_3) = \left(1, 0, -\sqrt{\frac{2a\lambda}{a+\lambda}}\right),$$
$$W = Im(v_3) = \left(0, \frac{2}{a+\lambda}\sqrt{\frac{a}{\lambda}}, \lambda\sqrt{\frac{2}{a+\lambda}}\right).$$

Using the vectors $2T, -2W$ and v_1 as columns, we construct the matrix

$$B = \begin{pmatrix} 2 & 0 & 1 \\ 0 & -2\beta^2\sqrt{\frac{a}{\lambda}} & -\frac{2}{\lambda} \\ -2\beta\sqrt{a\lambda} & -2\beta\lambda & \frac{2}{\beta}\sqrt{\frac{a}{\lambda}} \end{pmatrix},$$

where we denote $\beta = \sqrt{\frac{2}{a+\lambda}}$.

Considering the transformation

$$\begin{pmatrix} X \\ Y \\ Z \end{pmatrix} = B \cdot \begin{pmatrix} u \\ v \\ w \end{pmatrix},$$

that is

$$(T): \begin{cases} X = 2u + w \\ Y = -2\beta^2\sqrt{\frac{a}{\lambda}}v - \frac{2}{\lambda}w \\ Z = -2\beta\sqrt{a\lambda}u - 2\beta\lambda v + \frac{2}{\beta}\sqrt{\frac{a}{\lambda}}w \end{cases},$$

we get the normal form of system (7), namely

$$\begin{cases} \dot{u} = -\sqrt{a\lambda}v + F_1(u, v, w) \\ \dot{v} = \sqrt{a\lambda}u + F_2(u, v, w) \\ \dot{w} = -(a+\lambda)w + F_3(u, v, w) \end{cases}, \tag{8}$$

BUPT

where

$$
\begin{aligned}
F_1(u,v,w) &= \gamma A\left[-\beta^3 u - \frac{4\beta(\lambda-\beta^2)}{\lambda^2}\sqrt{\frac{a}{l}}v - \left(\frac{4(\lambda-\beta^2)}{\lambda^3\beta}+\frac{\beta^3}{2}\right)w\right] \\
&\quad - \frac{\gamma\beta^2}{2}\sqrt{\frac{a}{\lambda}}\,(2u+w)^2\,, \\
F_2(u,v,w) &= \gamma A\left[\beta\left(\frac{2}{\lambda}+\beta^2\right)\sqrt{\frac{a}{\lambda}}u + \frac{2\beta^3 a(\lambda-\beta^2)}{\lambda^2}v\right. \\
&\quad \left. + \left(\frac{\beta}{\lambda}+\frac{\beta^3}{2}+\frac{2\beta(\lambda-\beta^2)}{\lambda^2}\right)\sqrt{\frac{a}{\lambda}}w\right] - \frac{\gamma}{\lambda}\,(2u+w)^2\,, \\
F_3(u,v,w) &= \gamma A\left[2\beta^3 u - \frac{2a\beta^5(\lambda-\beta^2)}{\lambda^2}\sqrt{\frac{a}{l}}v - \left(\frac{2a\beta^3(\lambda-\beta^2)}{\lambda^2}-\beta^3\right)w\right] + \\
&\quad \gamma\beta^2\sqrt{\frac{a}{\lambda}}\,(2u+w)^2\,.
\end{aligned}
$$

We have denoted $\gamma = \left(\frac{4}{\lambda\beta}+a\beta^3\right)^{-1}$, and $A = -2\beta\sqrt{a\lambda}u - 2\beta\lambda v + \frac{2}{\beta}\sqrt{\frac{a}{\lambda}}w$.

By applying procedures and formulas proposed by Hassard [9], the aforementioned coefficients are given by:

$$
\begin{aligned}
g_{11} &= \frac{1}{4}\left[\frac{\partial^2}{\partial u^2}F_1 + \frac{\partial^2}{\partial v^2}F_1 + i\left(\frac{\partial^2}{\partial u^2}F_2 + \frac{\partial^2}{\partial v^2}F_2\right)\right], \\
g_{02} &= \frac{1}{4}\left[\frac{\partial^2}{\partial u^2}F_1 - \frac{\partial^2}{\partial v^2}F_1 - 2\frac{\partial^2}{\partial u\partial v}F_2 + i\left(\frac{\partial^2}{\partial u^2}F_2 - \frac{\partial^2}{\partial v^2}F_2 + 2\frac{\partial^2}{\partial u\partial v}F_1\right)\right], \\
g_{20} &= \frac{1}{4}\left[\frac{\partial^2}{\partial u^2}F_1 - \frac{\partial^2}{\partial v^2}F_1 + 2\frac{\partial^2}{\partial u\partial v}F_2 + i\left(\frac{\partial^2}{\partial u^2}F_2 - \frac{\partial^2}{\partial v^2}F_2 - 2\frac{\partial^2}{\partial u\partial v}F_1\right)\right], \\
h_{11} &= \frac{1}{4}\left[\frac{\partial^2}{\partial u^3}F_3 + \frac{\partial^2}{\partial v^3}F_3\right],\ h_{20} = \frac{1}{4}\left[\frac{\partial^2}{\partial u^3}F_3 - \frac{\partial^2}{\partial v^3}F_3 - 2i\frac{\partial^2}{\partial u\partial v}F_3\right], \\
w_{11} &= -\frac{h_{11}}{\mu_1}, w_{20} = \frac{h_{20}}{2i\alpha_0-\mu_1}, \\
G_{10} &= \frac{1}{2}\left[\frac{\partial^2}{\partial u\partial w}F_1 + \frac{\partial^2}{\partial v\partial w}F_2 + i\left(\frac{\partial^2}{\partial u\partial w}F_2 - \frac{\partial^2}{\partial v\partial w}F_1\right)\right], \\
G_{01} &= \frac{1}{2}\left[\frac{\partial^2}{\partial u\partial w}F_1 - \frac{\partial^2}{\partial v\partial w}F_2 + i\left(\frac{\partial^2}{\partial u\partial w}F_2 + \frac{\partial^2}{\partial v\partial w}F_1\right)\right], \\
G_{21} &= \frac{1}{8}\left[\frac{\partial^3}{\partial u^3}F_1 + \frac{\partial^3}{\partial u\partial v^2}F_1 + \frac{\partial^3}{\partial u^2\partial v}F_2 + \frac{\partial^3}{\partial v^3}F_2\right. \\
&\quad \left. + i\left(\frac{\partial^3}{\partial u^3}F_2 + \frac{\partial^3}{\partial u\partial v^2}F_2 - \frac{\partial^3}{\partial u^2\partial v}F_1 - \frac{\partial^3}{\partial v^3}F_1\right)\right], \\
g_{21} &= G_{21} + 2G_{10}w_{11} + G_{01}w_{20}.
\end{aligned}
$$

BUPT

where $\alpha_0 = \mathrm{Im}(\mu_3)$.

The first Lyapunov coefficient for E_1^- is given by

$$l_1(0) = \frac{1}{2a\lambda} Re\left(ig_{20}g_{11} + g_{21}\sqrt{a\lambda}\right), \tag{9}$$

where

$$\begin{aligned}
g_{11} &= \frac{\gamma}{\lambda}\left[\frac{\beta^2\sqrt{a}(\beta^2\lambda^2 - 4\beta^2 + 3\lambda)}{\sqrt{\lambda}} + i(2a\beta^6 - 3a\beta^4\lambda - 2a\beta^2 - 2)\right],\\
g_{02} &= \frac{\gamma}{\lambda}\left[\frac{-\beta^2\sqrt{a}(2a\beta^4 - 2a\beta^2\lambda - 2\beta^2\lambda^2 - 4\beta^2 + 3\lambda)}{\sqrt{\lambda}}\right.\\
&\quad \left. -i\left(\frac{2a\beta^6\lambda - a\beta^4\lambda^2 - \beta^4\lambda^3 + 4a\beta^4 - 2a\beta^2\lambda + 2\lambda}{\lambda}\right)\right],\\
g_{20} &= \frac{\gamma}{\lambda}\left[\frac{\beta^2\sqrt{a}(2a\beta^4 - 2a\beta^2\lambda + 4\beta^2 - 7\lambda)}{\sqrt{\lambda}}\right.\\
&\quad \left. -i\left(\frac{2a\beta^6\lambda - a\beta^4\lambda^2 + \beta^4\lambda^3 - 4a\beta^4 + 6a\beta^2\lambda + 2\lambda}{\lambda}\right)\right],\\
h_{11} &= -\frac{2\gamma\beta^2\sqrt{a}(a\beta^6 - a\beta^4\lambda + \beta^2\lambda - 1)}{\sqrt{\lambda}},\\
h_{20} &= \frac{\gamma}{\sqrt{\lambda}}\left[2\beta^2\sqrt{a}(a\beta^6 - a\beta^4\lambda - \beta^2\lambda + 1) + i\left(\frac{2\beta^4(a^2\beta^4 - a^2\beta^2\lambda + \lambda^2)}{\sqrt{\lambda}}\right)\right],\\
w_{11} &= \frac{\beta^2}{2}h_{11},\\
w_{20} &= \frac{\beta^2(1 - i\beta^2\sqrt{a\lambda})}{2(1 + a\lambda\beta^4)}h_{20},\\
G_{10} &= -\frac{\gamma\sqrt{a}(2a\beta^4 - 2\beta^4\lambda - 2a\beta^2\lambda + 5\beta^2\lambda^2 + 4\beta^2 - 4\lambda)}{\lambda^2\sqrt{\lambda}} -\\
&\quad i\left[\frac{\gamma(a\beta^4\lambda^3 + \beta^4\lambda^4 - 4a\beta^4\lambda + 4a\beta^2\lambda^2 + 8a\beta^2 - 8\beta^2\lambda - 12a\lambda + 12\lambda^2)}{2\lambda^3}\right],\\
G_{01} &= \frac{\gamma\sqrt{a}(\beta^4\lambda^3 + 2a\beta^4 - 2\beta^4\lambda - 2a\beta^2\lambda + \beta^2\lambda^2 - 4\beta^2 + 4\lambda)}{\lambda^2\sqrt{\lambda}} -\\
&\quad i\left[\frac{\gamma(a\beta^4\lambda^3 - \beta^4\lambda^4 - 4a\beta^4\lambda + 4a\beta^2\lambda^2 - 8a\beta^2 + 8\beta^2\lambda + 4a\lambda - 4\lambda^2)}{2\lambda^3}\right],\\
G_{21} &= 0,\\
g_{21} &= 2G_{10}w_{11} + G_{01}w_{20}.
\end{aligned}$$

BUPT

By using the same arguments and procedures as before, the stability of E_1^+ is analyzed. By the substitution

$$\begin{cases} x = -X + \sqrt{\dfrac{a}{1-g}} \\ y = -Y \\ z = Z + \dfrac{1}{1-g} \end{cases},$$

system (4) becomes (7). Therefore, we get the same first Lyapunov coefficient.

Taking into account the sign of $l_1(0)$, we obtain (ii) and the last assertion of (iii), which finishes the proof. □

4 Chaotic behavior

In this section, computer simulations point out the chaotic behavior of the system (4). In addition, evolutions of the largest Lyapunov exponent and the Kaplan - York dimension of the system (4) are analyzed.

Following [42], recall that the signs of the Lyapunov exponents give a qualitative picture of the dynamics of a system. The sum of the three Lyapunov exponents of a three-dimensional continuous dissipative dynamical system is negative, and consequently at least one Lyapunov exponent is negative. A positive Lyapunov exponent of a bounded attractor indicates the exponential expansion of the trajectory, hence "the system experiences repeated stretching and folding", which leads to a strange attractor.

The Lyapunov exponents μ_1, μ_2, μ_3 constitute the Lyapunov exponent spectrum, and their signs form the symbolic Lyapunov spectrum. For example, if $\mu_1 > 0, \mu_2 = 0, \mu_3 < 0$, then the corresponding element of the symbolic Lyapunov spectrum is the triple $(+, 0, -)$. "In a three-dimensional continuous dissipative dynamical system the only possible spectra, and the attractors they describe, are as follows: $(+, 0, -)$, a strange attractor; $(0, 0, -)$, a two-torus; $(0, -, -)$, a limit cycle; and $(-, -, -)$, a fixed point." [42]

In the sequel, we explore the variation of the largest Lyapunov exponent.

Consider the parameters a and λ fixed, namely $a = 0.45$, $\lambda = 0.75$. Using E&F Chaos program [5], in Figure 4, the variation of the largest Lyapunov exponent with respect to parameter g is presented. We can also see that the maximum value for the largest Lyapunov exponent is obtained for $g = 0.92$.

Now, we set the parameters $\lambda = 0.75$ and $g = 0.92$. In Figure 5, the variation of the largest Lyapunov exponent with respect to parameter λ is shown. In this case, the maximum value for the largest Lyapunov exponent is obtained for $a = 0.34$.

BUPT

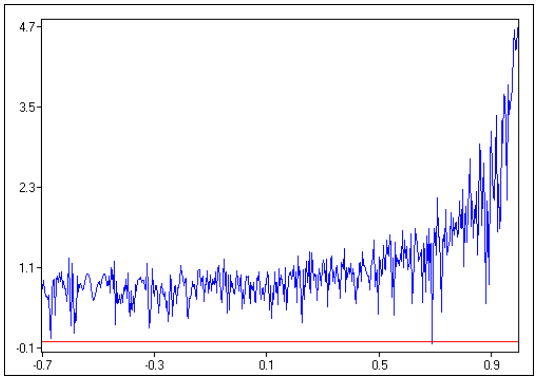


Figure 4: The variation of the largest Lyapunov exponent with respect to the parameter g ($a = 0.45$, $\lambda = 0.75$, $x_0 = 0.01$, $y_0 = 0.01$, $z_0 = 0.01$).

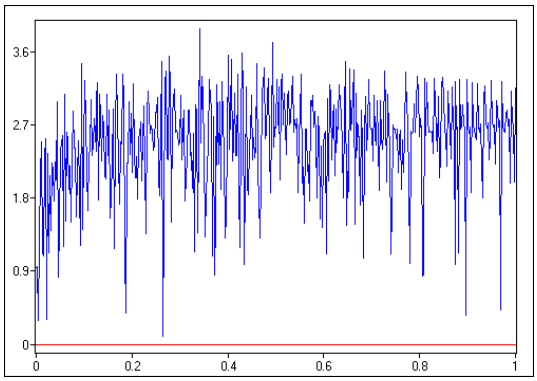


Figure 5: The variation of the largest Lyapunov exponent with respect to the parameter a ($\lambda = 0.75$, $g = 0.92$, $x_0 = 0.01$, $y_0 = 0.01$, $z_0 = 0.01$).

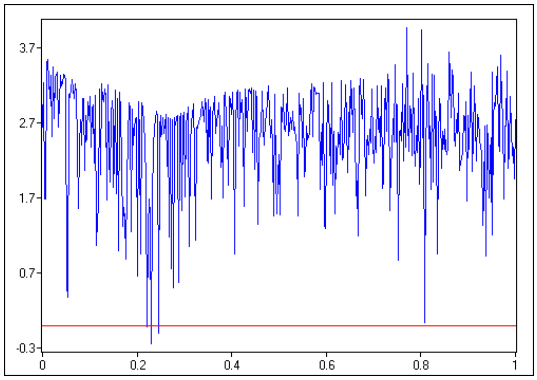


Figure 6: The variation of the largest Lyapunov exponent with respect to the parameter λ ($a = 0.45$, $g = 0.92$, $x_0 = 0.01$, $y_0 = 0.01$, $z_0 = 0.01$).

BUPT

Finally, in Figure 6, for $a = 0.45$ and $g = 0.92$, the variation of the largest Lyapunov exponent with respect to parameter λ is presented. In the last simulation, the maximum value for the largest Lyapunov exponent is obtained for $\lambda = 0.77$.

In the following we compare some chaotic indicators of the Shimizu-Morioka system and its deformation (4).

Recall that Shimizu-Morioka system (1) is chaotic for $a = 0.45, \lambda = 0.75$ (see, e.g., [33]). The corresponding attractor is drawn in Fig. 15(a).

Using "LCE package for Mathematica" [32], setting $a = 0.45$, $\lambda = 0.75$ and $g = 0$ in system (4) with the initial conditions $x_0 = 0.01$, $y_0 = 0.01$, $z_0 = 0.01$, the largest Lyapunov exponent is $\mu_1 = 0.0637008$. In addition, the other Lyapunov exponents are $\mu_2 \simeq 0$, $\mu_3 = -1.264$.

Setting $a = 0.34$, $\lambda = 0.77$ and $g = 0.92$ in system (4) with the initial conditions $x_0 = 0.01$, $y_0 = 0.01$, $z_0 = 0.01$, the largest Lyapunov exponent is $\mu_1 = 0.407006$. The other Lyapunov exponents are $\mu_2 \simeq 0$, $\mu_3 = -1.51811$.

The Lyapunov dimension or Kaplan–Yorke dimension of a chaotic attractor of a three-dimensional system is

$$D_L = 2 + \frac{\mu_1 + \mu_2}{|\mu_3|}.$$

Therefore $D_L = 2.05064$ for $a = 0.45$, $\lambda = 0.75$, $g = 0$ and $D_L = 2.26883$ for $a = 0.34$, $\lambda = 0.77$, $g = 0.92$

In Figure 7, the convergence plot of the Lyapunov spectrum for system (4) is presented.

Using Matlab R2023a, the time series (Fig. 8), the trajectory of the system (4) for $a = 0.34$, $\lambda = 0.77$, $g = 0.92$ (Fig. 9) and its projections on the coordinates planes (Fig. 10) are shown.

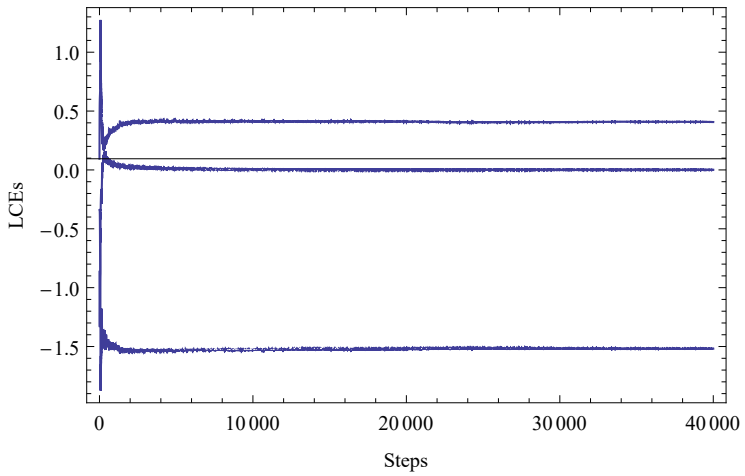


Figure 7: Convergence plot of the Lyapunov spectrum for system (4) ($a = 0.34$, $\lambda = 0.77$, $g = 0.92$, $x_0 = 0.01$, $y_0 = 0.01$, $z_0 = 0.01$).

BUPT

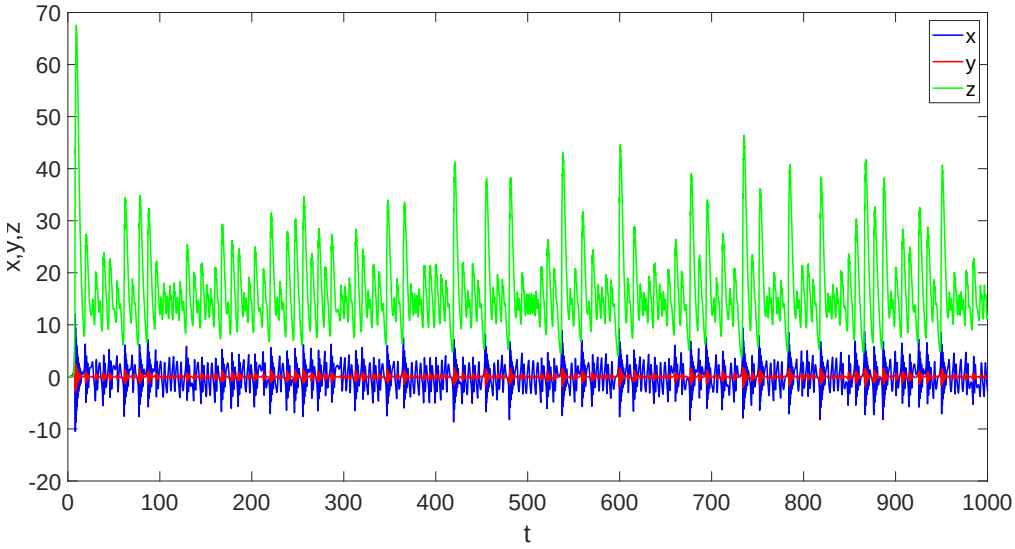


Figure 8: The time series of a chaotic attractor of system (4) for $a = 0.34$, $\lambda = 0.77$, $g = 0.92$, with the initial conditions $x_0 = 0.01$, $y_0 = 0.01$, $z_0 = 0.01$.

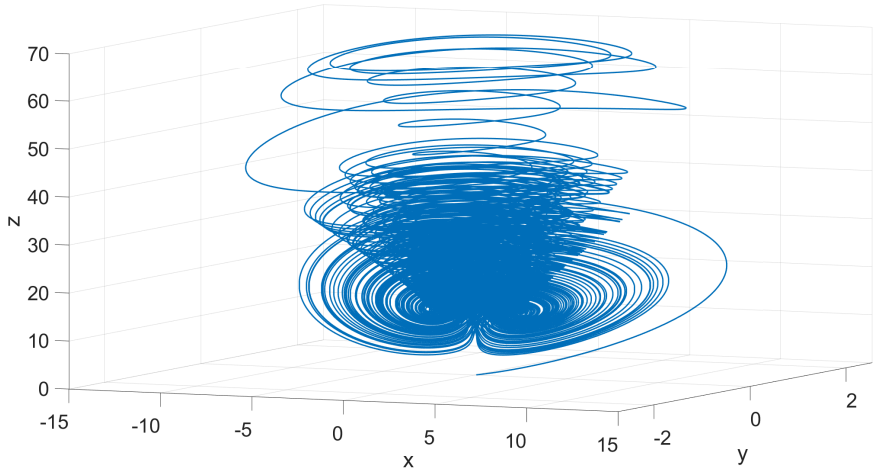


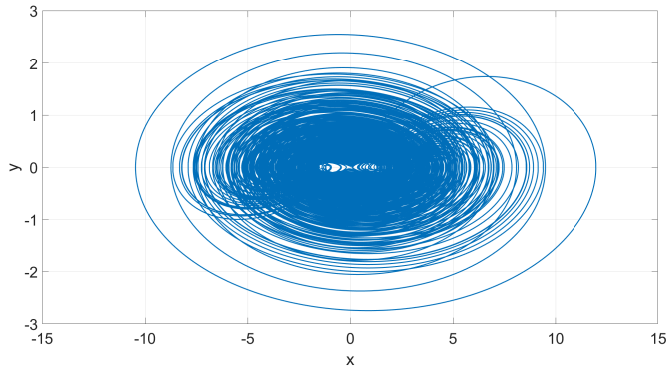
Figure 9: A chaotic attractor of system (4) for $a = 0.34$, $\lambda = 0.77$, $g = 0.92$, with the initial conditions $x_0 = 0.01$, $y_0 = 0.01$, $z_0 = 0.01$.

5 Numerical simulations

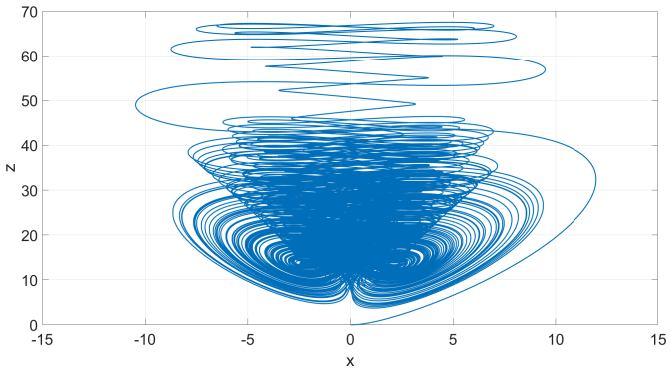
In this section, using Matlab R2023a, we give some numerical simulations of the trajectory of system (4) (see Figures 11-16).

We start with a route of chaos of the considered system in the case $a = 0.8$, $\lambda = 0.934$, and g varying between -0.8 and 0.9. An asymptotically stable attractor

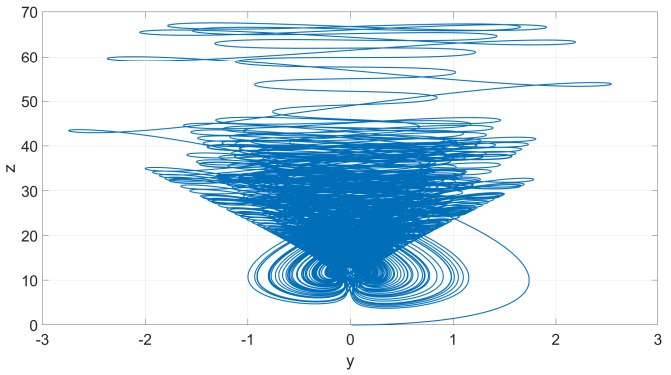
BUPT



(a) projection on the x-y plane



(b) projection on the x-z plane

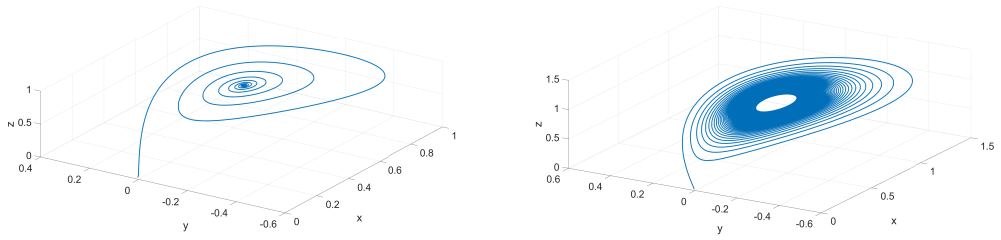


(c) projection on the y-z plane

Figure 10: The projections of the chaotic attractor of system (4) on the coordinates planes ($a = 0.34$, $\lambda = 0.77$, $g = 0.92$, $x_0 = 0.01$, $y_0 = 0.01$, $z_0 = 0.01$).

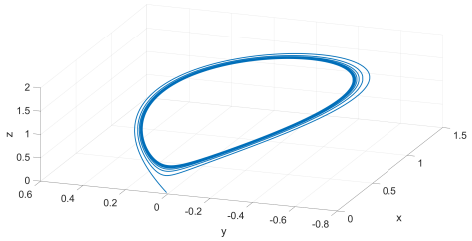
BUPT

(Fig. 11(a)) turns into a limit cycle (Fig. 11(b)), which is stable (Fig. 11(c)). This limit cycle deforms into a homoclinic orbit (Fig. 11(d)). Because system (4) has a rotational symmetry around $Oz-$axis, there is in fact a pair of homoclinic orbits, which give rise to a symmetric limit cycle (Fig. 11(e)), which is also stable (Fig. 11(f)). Note that these homoclinic orbits (in the case $g = 0$) were reported in [33]. The moment of the appearance of a strange attractor is shown in Fig. 12(b). The evolution of this attractor is presented in Figures 12(c)-12(h).

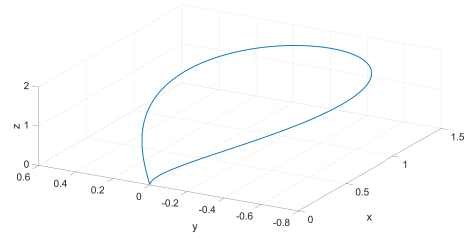


(a) $g = -0.8$

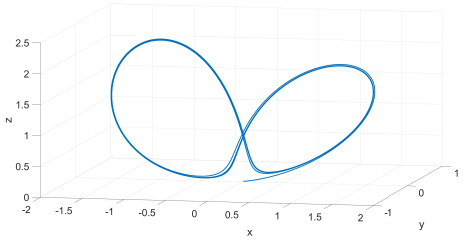
(b) $g = -0.2349$



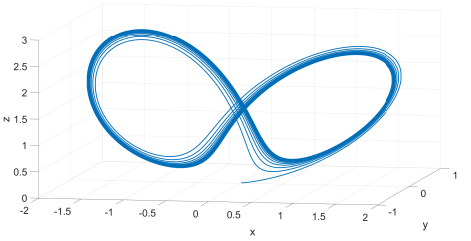
(c) $g = -0.1$



(d) $g = 0$



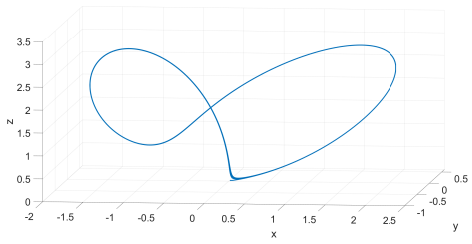
(e) $g = 0.1$



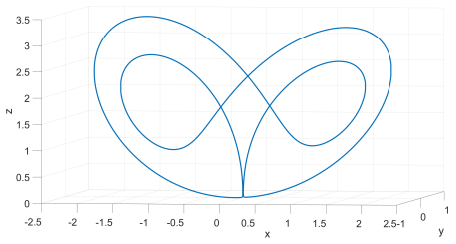
(f) $g = 0.3$

Figure 11: A deformation of system (4) ($a = 0.8$, $\lambda = 0.934$, $x_0 = 0.01$, $y_0 = 0.01$, $z_0 = 0.01$).

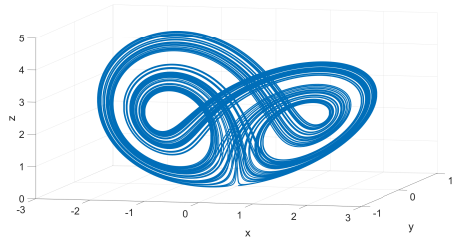
BUPT



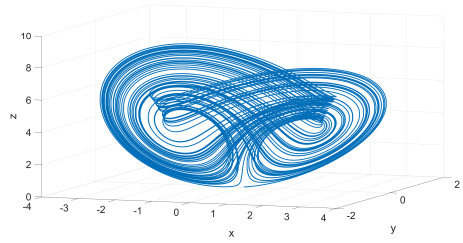
(a) $g = 0.38$



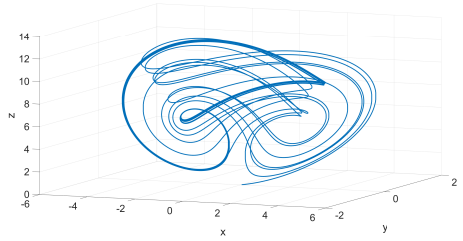
(b) $g = 0.383$



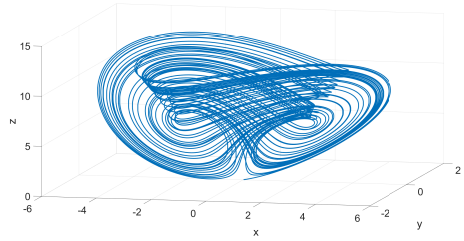
(c) $g = 0.5$



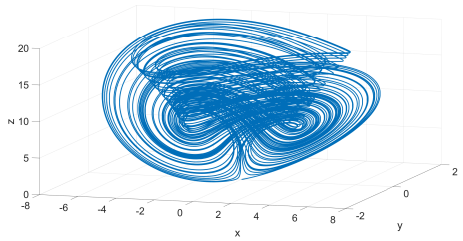
(d) $g = 0.7$



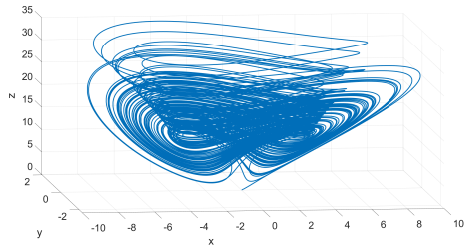
(e) $g = 0.798$



(f) $g = 0.799$



(g) $g = 0.85$



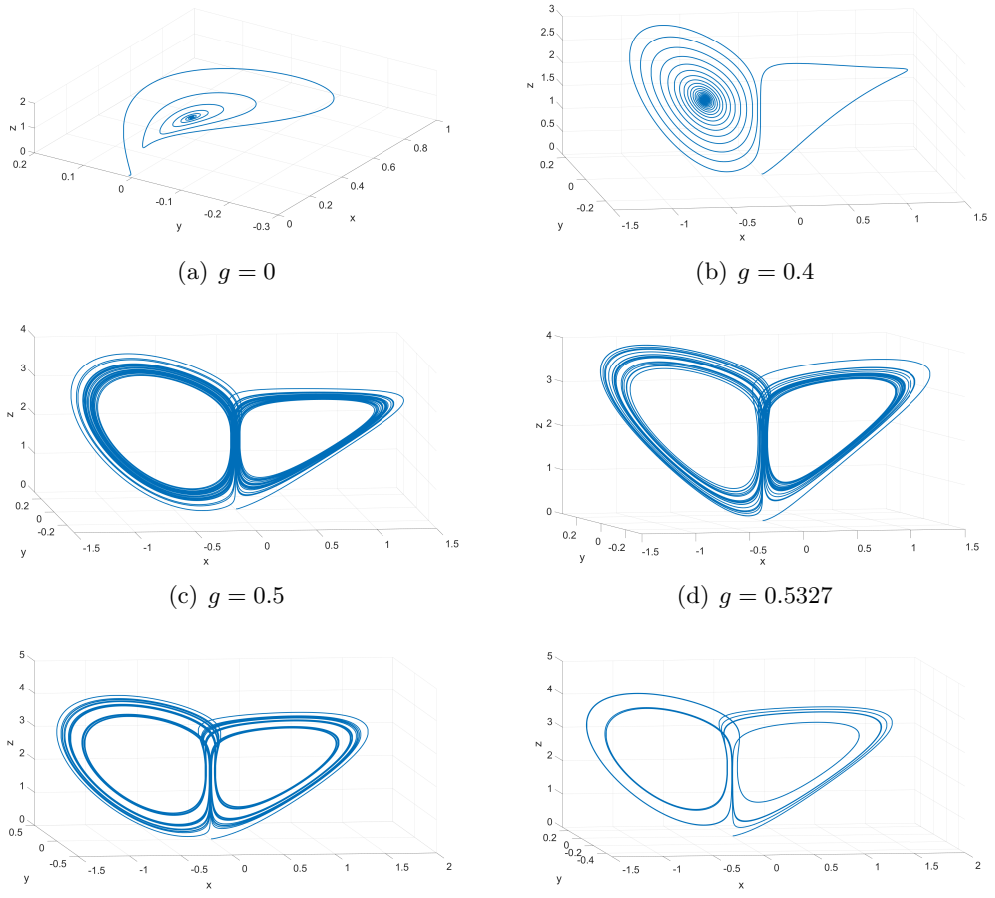
(h) $g = 0.9$

Figure 12: The continuation of Fig. 11: A deformation of system (4) ($a = 0.8$, $\lambda = 0.934$, $x_0 = 0.01$, $y_0 = 0.01$, $z_0 = 0.01$).

BUPT

Another transition between an asymptotically stable attractor and a strange attractor is presented in Figures 13 and 14. We set $a = 0.14$, $\lambda = 2$, and vary g between 0 and 0.9. For $g = 0$ system (4) has an asymptotically stable attractor (E_1^-, Fig. 13(a)) and before $g = 4$ it turns into another asymptotically stable attractor (E_1^+, Fig. 13(b)). Finally, another strange attractor is point out (Fig. 14(h)).

In Fig. 15, we present the transition of the Shimizu-Morioka chaotic attractor (Fig. 15(a)), which looks as the Lorenz attractor [27], to the new chaotic attractor (4) (Fig. 15(e)), which looks as the Chen attractor [4].



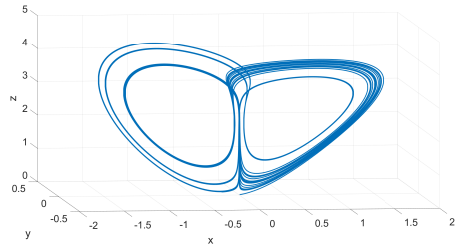
(a) $g = 0$ (b) $g = 0.4$

(c) $g = 0.5$ (d) $g = 0.5327$

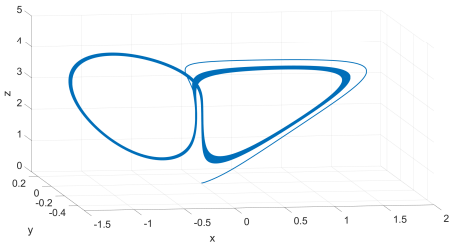
(e) $g = 0.56$ (f) $g = 0.57$

Figure 13: A deformation of system (4) ($a = 0.14$, $\lambda = 2$, $x_0 = 0.01$, $y_0 = 0.01$, $z_0 = 0.01$).

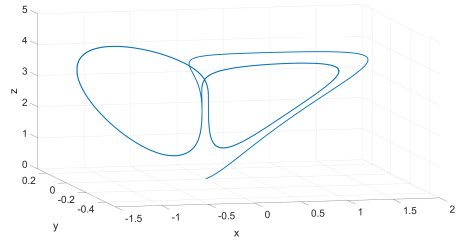
BUPT



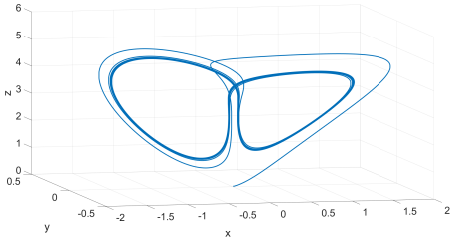
(a) $g = 0.58$



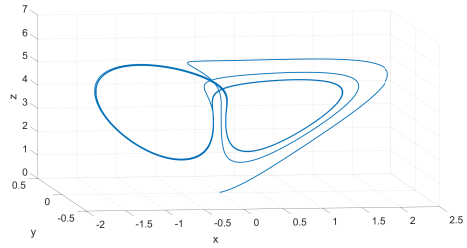
(b) $g = 0.59$



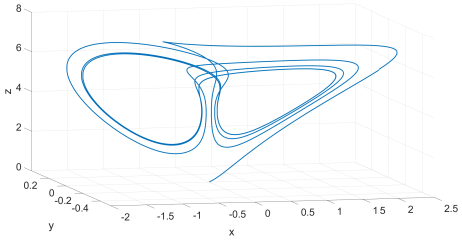
(c) $g = 0.6$



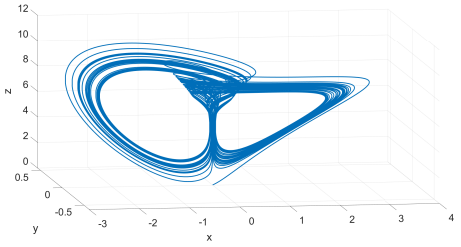
(d) $g = 0.65$



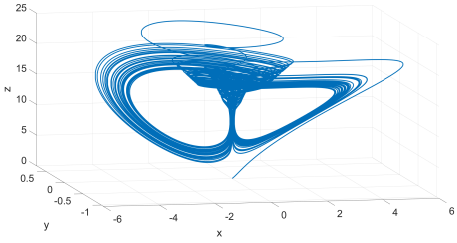
(e) $g = 0.7$



(f) $g = 0.75$



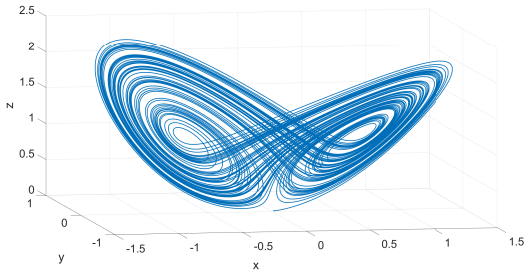
(g) $g = 0.8$



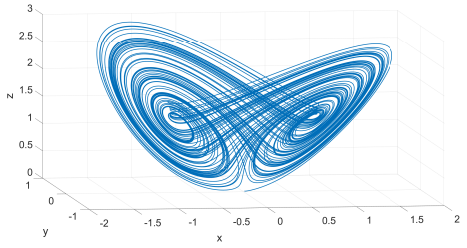
(h) $g = 0.9$

Figure 14: The continuation of Fig. 13: A deformation of system (4) ($a = 0.14$, $\lambda = 2$, $x_0 = 0.01$, $y_0 = 0.01$, $z_0 = 0.01$).

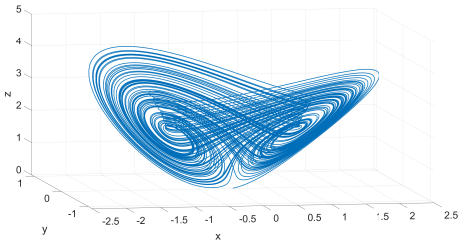
BUPT



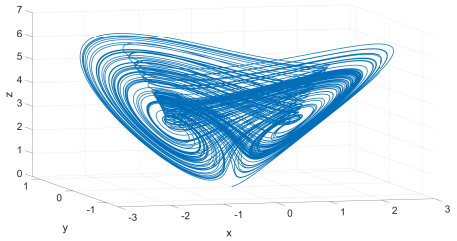
(a) $g = 0$



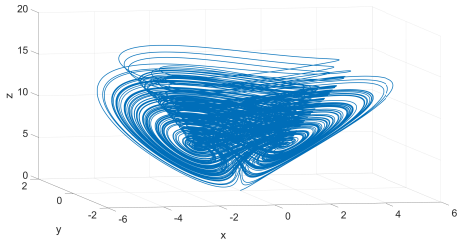
(b) $g = 0.2$



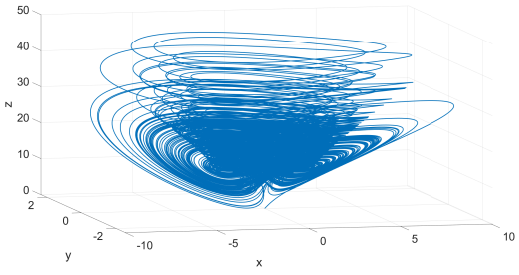
(c) $g = 0.4$



(d) $g = 0.6$



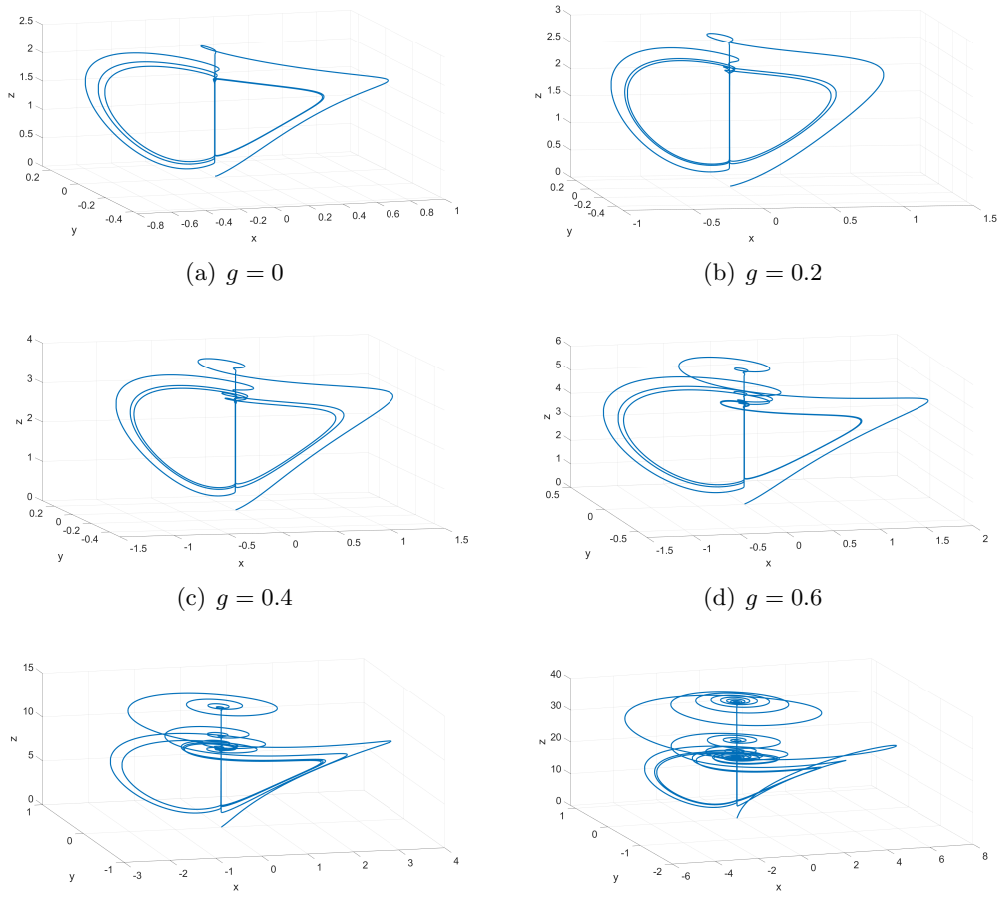
(e) $g = 0.8$



(f) $g = 0.9$

Figure 15: Deformations of the Shimizu-Morioka chaotic attractor (4) ($a = 0.45$, $\lambda = 0.75$, $x_0 = 0.01$, $y_0 = 0.01$, $z_0 = 0.01$).

BUPT



(a) $g = 0$ (b) $g = 0.2$

(c) $g = 0.4$ (d) $g = 0.6$

(e) $g = 0.8$ (f) $g = 0.9$

Figure 16: A chaotic deformation of system (4) for (a) $g = 0$; (b) $g = 0.2$; (c) $g = 0.4$; (d) $g = 0.6$; (e) $g = 0.8$; (f) $g = 0.9$. ($a = 0.01$, $\lambda = 1.4$, $x_0 = 0.01$, $y_0 = 0.01$, $z_0 = 0.01$).

References

[1] A. Babloyantz, C. Nicolis, J.M. Salazar, Evidence of chaotic dynamics of brain activity during the sleep cycle, *Physics Letters A*, **111**, (1985), 152–156.

[2] T. Bînzar, C. Lăzureanu, On a new chaotic system, *Mathematical Methods in the Applied Sciences*, **38**(8), (2015), 1631–1641.

[3] G. Chen, Controlling Chaos and Bifurcations in Engineering Systems, *CRC Press, Boca Raton, FL*, 1999.

[4] G. Chen, T. Ueta, Yet another chaotic attractor, *International Journal of Bifurcation and Chaos*, **9**, (1999), 1465–1466.

BUPT

[5] C. Diks, C.H. Hommes, V. Panchenko, R. van der Weide, E&F chaos: A user friendly software package for nonlinear economic dynamics, *Computational Economics*, **32**, (2008), 221—244.

[6] M.M. El-Dessoky, M.T. Yassen, E.S. Aly, Bifurcation analysis and chaos control in Shimizu-Morioka chaotic system with delayed feedback, *Applied Mathematics and Computation*, **243**, (2014), 283—297.

[7] A. Galajinsky, Remark on integrable deformations of the Euler top, *Journal of Mathematical Analysis and Applications*, **416**(2), (2014), 995–997.

[8] F.R. Gantmacher, *Matrix Theory*, Chelsea Pub. Co., New York, NY, USA, 2000, Volume 2.

[9] B. Hassard, Y.H. Wan, Bifurcation formulae derived from center manifold theory, *Journal of Mathematical Analysis and Applications*, **63**, (1978), 297–312.

[10] K. Huang, S. Shi, Z. Xu: Integrable deformations, bi-Hamiltonian structures and nonintegrability of a generalized Rikitake system, *International Journal of Geometric Methods in Modern Physics*, **16**(4), (2019), 1950059.

[11] K. Huang, S. Shi, W. Li., Integrability analysis of the Shimizu–Morioka system, *Communications in Nonlinear Science and Numerical Simulation*, **84**, (2020), 105101.

[12] W. Kinsner, Characterizing chaos through lyapunov metrics, *IEEE Transactions on Systems, Man and Cybernetics, Part C (Applications and Reviews)*, **36**(2), (2006), 141–151.

[13] Y.A. Kuznetsov, *Elements of Applied Bifurcation Theory*, Springer-Verlag: New York, NY, USA, 1998.

[14] C. Lăzureanu, On the Hamilton-Poisson realizations of the integrable deformations of the Maxwell-Bloch equations, *Comptes Rendus Mathematique*, **355**, (2017), 596–600.

[15] C. Lăzureanu, Hamilton-Poisson Realizations of the Integrable Deformations of the Rikitake System, *Advances in Mathematical Physics*, **2017**, (2017), 4596951.

[16] C. Lăzureanu, Integrable Deformations of Three-Dimensional Chaotic Systems, *International Journal of Bifurcation and Chaos*, **28**(5), (2018), 1850066.

[17] C. Lăzureanu, Chaotic behavior of an integrable deformation of a nonlinear monetary system, *AIP Conference Proceedings* 2116, (2019), 370004.

[18] C. Lăzureanu, Integrable Deformations and Dynamical Properties of Systems with Constant Population, *Mathematics*, **9**, (2021), 1378.

BUPT

[19] C. Lăzureanu, Dynamical Properties, Deformations, and Chaos in a Class of Inversion Invariant Jerk Equations, *Symmetry*, **14**, (2022), 1318.

[20] C. Lăzureanu, C. Căplescu, On a deformed version of the T system, *Proceedings of The XV-th International Conference on Mathematics and its Applications*, Timişoara, 2019, 90–97.

[21] C. Lăzureanu, C. Hedrea, C. Petrişor, Stability and some special orbits for an integrable deformation of the Rikitake system, *2018 International Conference on Applied Mathematics & Computer Science (ICAMCS)*, Paris, France, 2018, 1–18.

[22] C. Lăzureanu, C. Hedrea, C. Petrişor, On the integrable deformations of a system related to the motion of two vortices in an ideal incompressible fluid, *International Conference on Computational Methods and Applications in Engineering (ICCMAE 2018)*, Timişora, Romania, 2018, ITM Web of Conferences **29**, (2019), 01015.

[23] C. Lăzureanu, C. Petrişor, Stability and Energy-Casimir Mapping for Integrable Deformations of the Kermack-McKendrick System, *Advances in Mathematical Physics*, **2018**, (2018), 5398768.

[24] C. Lăzureanu, C. Petrişor, C. Hedrea, On a Deformed Version of the Two-Disk Dynamo System, *Applications of Mathematics*, **66**, (2021), 345–372.

[25] A.M. Lyapunov, *Problème Générale de la Stabilité du Mouvement*, Princeton University Press, Princeton, NJ, USA, 1949, Volume 17.

[26] J. Llibre, C. Pessoa, The Hopf bifurcation in the Shimizu-Morioka system, *Nonlinear Dynamics*, **79**, (2015), 2197–2205.

[27] E.N. Lorenz, Deterministic nonperiodic flow, *Journal of the Atmospheric Sciences*, **20**(2), (1963), 130–141.

[28] L.M. Pecora, T.L. Carroll, Driving systems with chaotic signals, *Physical Review A*, **44**(4), (1991), 2374–83.

[29] L. Perko, *Differential Equations and Dynamical Systems*, 3nd ed., Texts in Applied Mathematics 7, Springer-Verlag: New York, NY, USA, 2001.

[30] K. Pyragas, Continuous control of chaos by self-controlling feedback, *Physics Letters A*, **170**(6), (1992), 421–8.

[31] M.I. Rabinovich, H.D.I. Abarbanel, The role of chaos in neural systems, *Neuroscience*, **87**, (1998), 5–14.

[32] M. Sandri, LCE package for Mathematica 7, (2010), http://www.msandri.it.

BUPT

[33] A.L. Shil'nikov, On bifurcations of the Lorenz attractor in the Shimizu-Morioka model, *Physica D: Nonlinear Phenomena*, **62**(1-4), (1993), 338–346.

[34] T. Shimizu, N. Morioka, On the bifurcation of a symmetric limit cycle to an asymmetric one in a simple model, *Physics Letters A*, **76**(3-4), (1980), 201–204.

[35] J.C. Sprott, X. Wang, G. Chen, Coexistence of point, periodic and strange attractors, *International Journal of Bifurcation and Chaos*, **23**(5), (2013), 1350093.

[36] J.C. Sprott, A dynamical system with a strange attractor and invariant tori, *Physics Letters A*, **378**, (2014), 1361–1363.

[37] G. Tigan, Analysis of a dynamical system derived from the Lorenz system, *Scientific Bulletin of the Politehnica University of Timisoara*, **50**(**64**)(1), (2005), 61–72.

[38] G. Tigan, D. Turaev, Analytical search for homoclinic bifurcations in the Shimizu-Morioka model. *Physica D: Nonlinear Phenomena*, **240**(12), (2011), 985–9.

[39] X. Zhang, When Shimizu-Morioka model meets Jacobi stability analysis: Detecting chaos, *International Journal of Geometric Methods in Modern Physics*, **20**(2), (2023), 2350033.

[40] Z. Wei, J.C. Sprott, H. Chen, Elementary quadratic chaotic flows with a single non-hyperbolic equilibrium, *Physics Letters A* **2015**, *379*, 2184–2187.

[41] Z. Wei, X. Zhang, Chaos in the Shimizu-Morioka Model With Fractional Order, *Frontiers in Physics*, **9**, (2021), 636173.

[42] A. Wolf, J.B. Swift, H.L. Swinney, J.A. Vastano, Determining Lyapunov exponents from a time series, *Physica D: Nonlinear Phenomena*, **16**(3), (1995), 285–317.

Cristian Lăzureanu – Department of Mathematics,
Politehnica University of Timişoara,
P-ta Victoriei 2, 300 006, Timişoara, ROMANIA
E-mail: cristian.lazureanu@upt.ro

Jinyoung Cho – MSc student, Department of Mathematics,
Politehnica University of Timişoara,
P-ta Victoriei 2, 300 006, Timişoara, ROMANIA
E-mail: jinyoung.cho@student.upt.ro

BUPT